

Syracuse University

SURFACE

Physics

College of Arts and Sciences

2004

Drift-Mobility Measurements and Mobility Edges in Disordered Silicons

Eric A. Schiff
Syracuse University

Follow this and additional works at: <https://surface.syr.edu/phy>



Part of the [Physics Commons](#)

Recommended Citation

"Drift-mobility measurements and mobility-edges in disordered silicons," E. A. Schiff, *J. Phys.: Condens. Matter* 16, S5265-5275 (2004).

This Article is brought to you for free and open access by the College of Arts and Sciences at SURFACE. It has been accepted for inclusion in Physics by an authorized administrator of SURFACE. For more information, please contact surface@syr.edu.

Drift-mobility measurements and mobility edges in disordered silicons

E A Schiff

Department of Physics, Syracuse University, Syracuse, NY 13244-1130, USA

Received 26 August 2004, in final form 27 August 2004

Published 22 October 2004

Online at stacks.iop.org/JPhysCM/16/S5265

doi:10.1088/0953-8984/16/44/023

Abstract

Published electron and hole drift-mobility measurements in hydrogenated amorphous silicon (a-Si:H), amorphous silicon alloys (a-SiGe:H and a-SiC:H), and microcrystalline silicon ($\mu\text{c-Si:H}$) are analysed in terms of the exponential bandtail trapping model. A three-parameter model was employed using an exponential bandtail width ΔE , the band mobility μ_0 , and the attempt-to-escape frequency ν . Low-temperature measurements indicate a value around $\mu_0 = 1 \text{ cm}^2 \text{ V}^{-1} \text{ s}^{-1}$ for both the conduction and valence bands over the entire range of materials. High temperature-measurements for electrons in a-Si:H suggest a larger value of $7 \text{ cm}^2 \text{ V}^{-1} \text{ s}^{-1}$. These properties and those of the frequency ν are discussed as possible attributes of a mobility edge.

1. Introduction

Over the last three decades, experimental characterizations of electrical transport in disordered semiconductors and insulators have accreted substantially. There is a particular accretion depth for hydrogenated amorphous silicon (a-Si:H) and related materials. Primarily because amorphous silicon has become an industrially significant material, we now know a great deal about the distinctions between different types of a-Si:H, about the effects of alloying of a-Si:H with Ge (a-SiGe:H) and C (a-SiC:H), and about ‘mixed phase’ nanocrystalline aggregates ($\mu\text{c-Si:H}$) that are primarily crystalline, but are deposited using the same apparatus as a-Si:H.

In this paper we discuss the photocarrier drift-mobility measurements in a-Si:H and other closely related ‘disordered silicons’; such measurements are generally based on observations of the time of flight required for a photocarrier distribution to drift between two electrodes in an electric field. For disordered semiconductors the time dependence of carrier drift is often anomalous, in the sense that the displacement $x(t)$ is not proportional to the time interval since the carriers were generated. This type of transport could only be analysed properly once Scher, Lax, and Montroll introduced the ideas of ‘dispersive transport’ in the mid-1970s (see Scher *et al* 1991).

One of the important early surprises for a-Si:H was that the drift-mobility measurements could be described well by a phenomenological trapping model (Tiedje *et al* 1981). The fundamental concept was that of a transport edge dividing the electronic density of states into ‘transport’ states with level energies on one side of the edge and ‘traps’ with level energies on the other. The traps are distributed as a ‘bandtail’ that tails away, often exponentially, into the gap of the semiconductor. Of course, the very existence of a bandgap in non-crystalline materials was a theoretical puzzle to physicists until Thorpe and Weaire (1971); Weaire and Thorpe (1971) showed that it made sense for certain models of covalent solids. The bandtail width ΔE is now often viewed as indicating the extent of the disorder in the semiconductor. The transport states are characterized by a band mobility μ_0 .

This paper is a re-examination of the trapping parameters that emerge from many of the previous measurements of electron and hole drift mobilities in disordered silicons. To improve the consistency of the parameters, we have re-analysed all the measurements using a unified set of procedures. The main result is that the electron and hole band mobilities μ_0 in a wide range of disordered silicon materials are reasonably consistent with a universal value around $10^{0.5} \text{ cm}^2 \text{ V}^{-1} \text{ s}^{-1}$; while this result has been proposed or suspected before, we find that this value describes a surprisingly large range of materials: a-Si:H of several varieties, a-SiGe:H, and at least some samples of $\mu\text{C-Si:H}$.

A secondary result concerns the ‘attempt-to-escape’ frequency ν , which appears as the prefactor in the assumed emission rate $\nu \exp(-(E - E_C)/k_B T)$ that describes emission of a carrier from a trap with level energy E to the transport edge (at level E_C). For electrons and the conduction bandtail, we find apparently random variations around a magnitude of 10^{11} – 10^{12} s^{-1} for a range of bandtail widths from 20–40 meV. For holes and the valence bandtail, we find a decrease in this parameter by a factor of about 1000 as the valence bandtail narrows from 50 to 30 meV.

Most workers have presumed that the transport edge is actually Mott’s ‘mobility edge’ that separates delocalized and localized electronic states (see Mott 1987). It turns out that pure-hopping models involving only localized states in bandtails also yield drift mobilities that are largely consistent with experiments, so some ambiguity still attaches to the nature of the transport edge. To the best of our knowledge, there are no theoretical explanations at present for any of these results: a universal value for μ_0 , its proposed magnitude, or the variations in ν . We discuss some of the possibilities in the concluding section of this paper.

2. Photocarrier trapping and drift experiments

Experimentally, the bandtail and the transport-edge ideas are employed to describe transient measurements on a group of excess electrons that are initially in states above E_C (or of excess holes below E_V). Such a group can be photogenerated using a short laser pulse that excites electrons from the valence band to the conduction band. There are several excellent introductions to this type of experiment and its interpretation (Tiedje 1984, Marshall 1989, Street 1991, Könenkamp 2000); in order to make the present paper reasonably self-contained, we briefly summarize the main issues.

Picosecond optical studies indicate that the resulting electron distribution, which initially occupies levels well above the edge E_C of the conduction band, thermalizes within the states above E_C very rapidly (within picoseconds; Nampoothiri *et al* 2003, Moon *et al* 1994). One presumes that electrons have adopted a Boltzmann distribution above E_C that is characterized by the sample’s lattice temperature. Analogous ideas describe the thermalization of holes following their photogeneration.

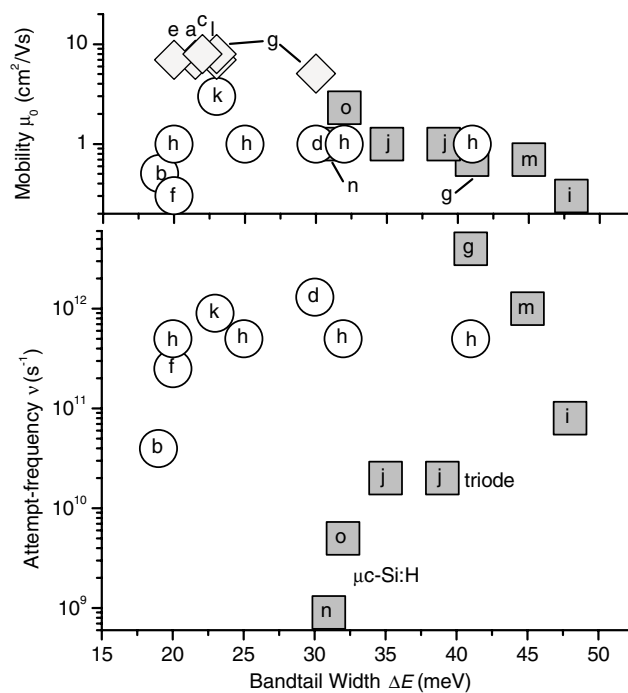


Figure 1. Mobility and trapping parameters for electron and hole drift-mobility experiments in a-Si:H, a-SiGe:H, and $\mu\text{c-Si:H}$. The upper panel shows band mobility parameters μ_0 plotted as a function of the exponential bandtail width ΔE (conduction bandtail for electrons, valence bandtail for holes). The lower panel shows the attempt-to-escape frequencies ν as a function of ΔE . The diamond symbols (lightly shaded) indicate conduction band mobilities for $1/T = 0$ based on extrapolation of high-temperature electron measurements in a-Si:H ($k_B T > \Delta E$). Circles and squares (shaded) indicate estimates from low-temperature measurements for electrons and holes, respectively. The low-temperature model ($k_B T < \Delta E$) assumes a temperature-independent band mobility. The letter for each symbol indicates its reference; the key is given in table 1.

Thermalization within the localized bandtail states is much slower, particularly at lower temperatures. There must be an initial trapping phase when the photocarrier distribution falls into the bandtail. The subsequent evolution is dominated by the thermally activated emission of carriers from the bandtail traps back to the transport states; the emission rate is assumed to be $\nu \exp(-(E - E_C)/k_B T)$, where E is the energy of the trapped carrier and ν is the ‘attempt-to-escape’ frequency. Once emitted, a carrier of course re-traps; the cycle of trapping, emission, re-trapping, re-emission, etc is termed ‘multiple trapping’. Ultimately, the excess photocarriers either leave the sample (the time-of-flight experiment), or recombine with their countercharges.

Optical techniques can probe these thermalization processes well, but the most common experiment is to apply an electric field and then measure the photocurrent due to motion of the thermalizing photocarrier distribution. In the absence of trapping, the distribution moves with a drift velocity $v = \mu_0 F$, where F is the electric field and μ_0 is the band mobility. Trapped carriers are usually considered to be immobile, so the photocurrent in the presence of trapping is determined both by the band mobility and by the fraction of carriers in transport states.

3. Mobility and trapping parameters in disordered silicons

Figure 1 presents the bandtail trapping parameters for many of the drift-mobility experiments published in the last 20 years or so. In several cases the parameters differ from those in the

Table 1. Key to the letter codes (a–o) used in figure 1 to identify the experimental references for the trapping parameter graphs.

Code	Description	Reference
a	a-Si:H; e	Hourd and Spear (1985)
b	a-Si:H; e	Marshall <i>et al</i> (1986)
c	a-Si:H; e	Street <i>et al</i> (1988)
d	a-SiGe:H; e, h	Nebel <i>et al</i> (1988)
e	a-Si:H; e	Devlen <i>et al</i> (1989)
f	a-SiGe:H; e	Longeaud and Vanderhagen (1990)
g	a-SiGe:H; e, h	Nebel (1991)
h	a-SiGe:H; e	Wang <i>et al</i> (1993)
i	a-Si:H and a-SiC:H; e, h	Gu <i>et al</i> (1994)
j	Triode a-Si:H; h	Ganguly <i>et al</i> (1995), Rao (1999)
k	a-Si:H; e	Gu <i>et al</i> (1995)
l	a-Si:H; e	Juška <i>et al</i> (1995)
m	a-Si:H; h	Dinca <i>et al</i> (2003)
n	Microcrystalline Si:H; h	Dylla <i>et al</i> (2004)
o	Microcrystalline Si:H; h	Dylla (2004)

original references; in these cases we have re-analysed the measurements so that a common fitting procedure has been applied for all the experiments. We have separately graphed the dependences of the band mobility μ_0 and the attempt-to-escape frequency ν upon the (exponential) bandtail width ΔE . Each symbol represents a different sample; the letter within or near each symbol indicates the reference for each measurement according to the key in table 1. The open symbols indicate results for electrons; the symbols with darker, shaded interiors indicate results for holes. The different shapes of the symbols indicate one of three types of experiment. The diamonds indicate results from high-temperature experiments on electrons in a-Si:H and a-SiGe:H, where high temperatures are defined as $k_B T > \Delta E$. The circles indicate results for electrons from low-temperature measurements. Note that the wider conduction bandtail widths (>25 meV) correspond to a-SiGe:H. The squares indicate results for holes from low-temperature regime measurements.

3.1. Parameters from high-temperature experiments

The most important estimates of the band mobility μ_0 are those obtained in the high-temperature regime ($k_B T > \Delta E$). At these temperatures, bandtail trapping is a relatively weak effect, and thus the measured drift mobilities have the same magnitude as μ_0 . For low-temperature measurements ($k_B T < \Delta E$), bandtail trapping reduces the drift mobilities by as much as several orders of magnitude from μ_0 , and the errors in obtaining μ_0 by parameter fitting are much larger.

High-temperature drift mobilities have been reported only for electrons. For electrons, the high-temperature regime corresponds to temperatures at room temperature and above, since the typical conduction bandtail width $\Delta E \sim 20$ meV; since the valence bandtail is generally broader than the conduction bandtail, much higher temperatures would be required to measure holes. Several experiments are indicated using the open, diamond symbols in figure 1; the temperatures studied ranged from 250 to 450 K. The bandtail widths in these experiments were obtained from low-temperature experiments for each experiment; the procedure for determining this parameter will be discussed subsequently.

The high-temperature measurements on electrons can be fitted well to the form

$$\mu_d(T) = \mu_0(1 - T_0/T)(k_B T > \Delta E). \quad (1)$$

The values of μ_0 in figure 1 are based on this fitting. The fitting parameter T_0 has a value similar to $\Delta E/k_B$ (about 250 K) in all the experiments. All the experiments yielded estimates of μ_0 of about $7 \text{ cm}^2 \text{ V}^{-1} \text{ s}^{-1}$. It is important to note that the drift-mobility measurements did not exceed $4 \text{ cm}^2 \text{ V}^{-1} \text{ s}^{-1}$ in these experiments; the parameter μ_0 represents the extrapolated drift mobility at $T = \infty$ in equation (1). It is remarkable how well these completely independent experiments agree with each other—especially when it is considered that the differing experiments correspond to timescales ranging from picoseconds to nanoseconds.

3.2. Trapping models for the high-temperature drift mobility

Equation (1) was obtained fairly early from a bandtail trapping model (Tiedje 1984). In trapping models, the drift mobility is calculated from the expression

$$\mu_d = \mu_0 \frac{n_c}{n_c + n_t}, \quad (2)$$

where n_c is the density of photoexcited carriers above the transport edge and n_t is the density of carriers trapped below the edge. The temperature dependence in equation (1) was obtained assuming a density of states $g(E)$ that is constant above the transport edge, and exponential below this edge. For high temperatures ($k_B T > \Delta E$), we can assume that the distribution of electrons within the conduction band $g(E)$ is fully thermalized, and n_c and n_t are calculated by assuming an exponential (Boltzmann) occupancy for the specified $g(E)$. The temperature dependence of equation (1) is just due to the ratio of the electron densities above and below the transport edge.

The success of this calculation just given is peculiar. There is no theoretical justification of which we are aware for the form of $g(E)$ that was assumed, which has a discontinuous derivative at the transport edge. A more refined trapping model based on a linear $g(E)$ at the transport edge, usually with an exponential form for deeper-lying states in the bandtails, also fits the high-temperature measurements satisfactorily (Marshall *et al* 1986, Street *et al* 1988, Nebel and Bauer 1989). However, the main difficulty with the trapping calculations is that they do not incorporate the temperature dependence of the conduction bandtail width that was subsequently reported in this same temperature regime by Aljishi *et al* (1990).

In these photoemission experiments at high temperatures ($k_B T > 25 \text{ meV}$), the conduction bandtail width ΔE was reported to be proportional to the absolute temperature. Recent computational work on the density of states is qualitatively consistent with this result (Atta-Fynn *et al* 2004), as were older optical absorption experiments showing that the valence bandtail width also increases (for even higher temperatures Cody *et al* 1982).

A temperature-dependent bandtail violates a basic assumption of trapping models, which is a well defined density of states that is independent of experimental variables. Interestingly, for two phosphorus-doped samples, Aljishi *et al* (1990) found that the conduction bandtail width was constant below a ‘freeze-in’ temperature around 350 K. They speculated that their undoped sample would have shown ‘freeze-in’ as well, but at a lower temperature than their experimental minimum (about 300 K). This speculation would account for the success of trapping models at lower temperatures in undoped a-Si:H, which we shall discuss shortly.

To the best of our knowledge, there has been no effort to connect the high-temperature drift-mobility measurements with the photoemission work, despite the fact that the two experiments covered the same range of temperatures. It should be noted that strict quantitative agreement cannot be expected; the photoemission work is sensitive only to the top 10–20 nm of a specimen, whereas the drift mobility represents an average of sample properties over a range of 500 nm or more. Nonetheless, it seems probable that the explanation of equation (1) based on a standard trapping model is inadequate. We discuss one alternative in the concluding section.

3.3. Bandtail multiple-trapping model at low temperatures

We noted in the introduction that, at low temperatures $k_B T < \Delta E$, drift-mobility measurements are ‘dispersive’, and in many cases have been described successfully using bandtail multiple-trapping models. In multiple-trapping models, the mobile-carrier ratio on the right-hand side of equation (2) is time dependent; the system has a memory of the photogeneration of the carriers at $t = 0$. Analyses of the multiple-trapping equations have been presented many times, and we refer the reader to the standard references (Arkhipov and Rudenko 1982, Rudenko and Arkhipov 1982, Orenstein *et al* 1982, Tiedje 1984) for these. Most experimenters analyse their measurements with approximate analytical solutions; the approximate solutions have been checked against exact numerical solution and Monte Carlo computer simulations in several cases (Marshall 1989, Chen and Hamel 1996). One such approximate analytical solution (Dinca *et al* 2003) is the following:

$$x(t)/F = K(\mu_0/v)(vt)^\alpha \quad (3)$$

$$K \equiv \sin(\alpha\pi)/(\alpha\pi(1-\alpha)) \quad \alpha \equiv k_B T/\Delta E < 1. \quad (3a)$$

Here $x(t)$ is the mean displacement of the photocarrier distribution since its photogeneration at $t = 0$, and F is the electric field inducing the displacement. The parameter α is termed the ‘dispersion’ parameter. When $\alpha \geq 1$, electrical transport of the photogenerated carriers is normal or ‘Gaussian’, and the displacement $x(t)$ is proportional to time. Values of $\alpha < 1$ are common in disordered semiconductors, in which case the displacement sublinearly with time; this type of transport is termed ‘dispersive’. The hallmark of bandtail multiple-trapping is that the dispersion parameter α is proportional to temperature (see equation (3a)).

While the form of equation (3) is very well accepted, the function K depends on the assumed form for $g(E)$ near E_C . K is of order unity; the particular expression for K in equation (3a) assumes that the transport edge lies within the exponential bandtail.

Most experimenters measure transit times t_T corresponding to photocarrier displacement across the sample’s thickness. It is conventional to report transit time measurements in terms of average drift mobilities μ_D that are calculated from the definition $\mu_D \equiv L/Ft_T$; here L is the displacement of the photocarrier distribution and F is the electric field. In terms of the multiple-trapping solution in equation (3), the transit time is determined implicitly from the equality $x(t_T) = L$, from which one calculates the bandtail trapping expression for the average drift mobility:

$$\mu_D = \left(\frac{Lv}{F}\right)^{1-1/\alpha} (K\mu_0)^{1/\alpha}. \quad (4)$$

Note that, for dispersive transport, there is a dependence of μ_D upon the electric field F ; this dependence does not imply nonlinear transport; the displacement of the carriers in a given time is still proportional to the field F . We note also that there is an unresolved inconsistency in the experimental literature regarding the relationship of the displacement L and the sample thickness d at the transit time; we believe $L = d/2$ is usually correct for dispersive measurements, but most authors use $L = d$.

In figure 1, the circular and square symbols correspond to parameters fitted to low-temperature measurements using either equation (3) or (4). Several authors have used more complex multiple-trapping models with additional parameters. One goal of these more complex analyses has been to obtain a single form encompassing both low- and high-temperature behaviour, but as we noted above it is not clear that this goal can be achieved in a pure trapping model.

Drift-mobility measurements on some materials cannot be successfully described using exponential bandtail multiple trapping (Nebel and Bauer 1989, Brinza *et al* 2004). These measurements, which include some of our own, are of course not included in the figure. Two principal mechanisms that have been advanced for a breakdown in exponential bandtail multiple-trapping are a non-exponential form for the bandtail density of states (Marshall *et al* 1986, Nebel and Bauer 1989, Brinza *et al* 2004) and also ‘hopping down’ transport (Monroe 1991, Shklovskii *et al* 1989) that bypasses the transport edge.

3.4. Parameters from low-temperature experiments (electrons)

The circular symbols in figure 1 are parameters obtained for electron drift-mobility measurements in varying forms of a-Si:H prepared by many laboratories. The differences in the materials can be readily discerned from the range of the conduction bandtail widths (from about 20 to 40 meV). Especially for electrons, it is helpful to simultaneously consider the alloying of a-Si:H with Ge. Ge alloying narrows the optical bandgap; much of the interest in Ge alloying originates from the possibility of using this effect to optimize the optical absorption properties of materials in solar cells. Ge alloying also broadens the conduction bandtail width fairly strongly (by about 20 meV in figure 1). Wang *et al* (1993) reported a roughly linear relationship between the broadening of bandtail width and the narrowing of the optical gap.

Earlier, Cody *et al* (1982) had reported a linear relationship between the valence bandtail width (from optical measurements—i.e. the ‘Urbach’ tail) and the bandgap for samples with varying deposition temperatures or with the measurement temperature. Cody *et al* envisioned a superposition of static and thermal ‘disorder’. Similarly, one might attribute the alloying effect on the conduction bandtail to an increase in ‘chemical disorder’ of the material; one imagines random, substitutional disorder in the bonding network of the amorphous solid adding to the effects of the non-crystalline network itself.

The conduction band mobility parameters μ_0 based on the low-temperature measurements are typically about $1 \text{ cm}^2 \text{ V}^{-1} \text{ s}^{-1}$. This value is distinctly smaller than the results from the high-temperature studies; we speculate regarding the origin of this difference in the concluding section. The conduction band attempt frequencies range from about 10^{11} to 10^{12} s^{-1} ; we will discuss this estimate after the hole measurements are presented in the next section.

It is worth noting that alloying a-Si:H with C increases the bandgap and decreases the electron drift mobility (Gu *et al* 1994, Bayley and Marshall 1996, Schmidt *et al* 2000)—a sort of ‘inverse Cody effect’. Full, three-parameter fits to the bandtail multiple-trapping equations had rather larger errors, and were not included in figure 1. Liu *et al* (1992) were able to measure the electron drift mobility of samples of a-Ge:H (unalloyed with Si); while the drift mobilities themselves were only modestly lower than for 50% alloys, and participated in the same broad trends, the authors were unsuccessful with bandtail multiple trapping. We were unable to obtain satisfactory three-parameter fits to the a-SiGe:H alloy sample studied by Longeaud and Vanderhagen (1990); as for the work of Liu *et al* the electron drift mobility itself was reasonably consistent with the other work on Ge alloying that we have summarized in figure 1.

3.5. Parameters from low-temperature experiments (holes)

The properties of holes in disordered silicons are not as well explored as the properties of electrons, but there has been a spate of recent activity. The measurements for which we have been able to calculate bandtail multiple-trapping parameters using equations (3) or (4) are presented as the shaded square symbols in figure 1. Three fairly different types of material are represented. a-Si:H valence bandtail widths are in the range 45–50 meV, and are otherwise

unlabelled. The tantalizing ‘triode-deposited’ materials of Ganguly *et al* (1995) are indicated, with a bandtail width of about 37 meV; for these materials, we confirmed the hole drift-mobility measurements and independently estimated the multiple-trapping parameters (Rao 1999). Finally, we present some very recent work based on hole drift-mobility measurements in two ‘microcrystalline’ $\mu\text{c-Si:H}$ samples (Dylla *et al* 2004, Dylla 2004). Raman spectroscopy indicates that about 60% of the volume of these material is ‘crystalline,’ but valence bandtail multiple trapping still applies. The valence bandtail width of about 30 meV is much smaller than the valence bandtail width for a-Si:H, but remains larger than typical conduction bandtail widths in a-Si:H. Some earlier work on drift mobilities in other $\mu\text{c-Si:H}$ materials was not consistent with bandtail multiple trapping, and has not been included (Juška *et al* 2001).

These hole measurements yield valence band mobility parameters μ_0 with the same magnitude as the low-temperature results for electrons, and tend to suggest that this value is a universal property of the transport edge. On the other hand, the variation in the valence bandtail attempt frequency ν is much larger than the alloying-induced changes for the conduction bandtail.

There has been little published on alloying effects for hole drift mobilities. The paper by Gu *et al* (1994) reported little dependence of the hole drift mobility on either C or Ge alloying, but more recent and extensive work (Schmidt *et al* 2000) found a sizable effect for C alloying.

Another fascinating experiment that is not included in figure 1 measured hole drift mobilities in compensated a-Si:H (Howard and Street 1991). The samples were prepared with P and B dopants at equal (effective) densities so that the conductivity of the samples remained very low, but the compensating, large densities of bonded P^+ and B^- ions introduced additional electrostatic fluctuations into the material beyond those that are intrinsic to the non-crystalline state. The authors concluded that disorder-induced bandtail states did not explain the mobility measurements in compensated samples, and suggested that the drift mobility was limited by long-range potential fluctuations.

4. Discussion

4.1. Low-temperature estimates of μ_0

We first discuss the meaning of a possible ‘universal’ value for the band mobility μ_0 . A value around $1 \text{ cm}^2 \text{ V}^{-1} \text{ s}^{-1}$ was obtained from low-temperature measurements for a wide variety of samples, and for both electrons and holes. Such a universal mobility value is not an obvious implication of Mott’s discussion of mobility edges (see Mott (1987) and references therein); Mott had proposed that the product $N_{\text{C}}e\mu_0$ at a mobility edge should have a value of a minimum metallic conductivity σ_{min} , where N_{C} is the ‘effective density of states’ of the conduction band. The minimum metallic conductivity is of order $\sigma_{\text{min}} \approx e^2/\hbar a$, where a is a typical bond length. Assuming that a is about 0.3 nm in Si, Mott suggested a value $\sigma_{\text{min}} \approx 10^3 \Omega^{-1} \text{ cm}^{-1}$.

If the minimum metallic conductivity idea were valid for these experiments, the subsidiary implication of the near constancy of μ_0 in figure 1 is that N_{C} and also N_{V} are each also constant, independent of variations both in ΔE and in ν , and with a magnitude of 10^{21} – 10^{22} cm^{-3} . Since there are no definitive experimental measurements of N_{C} and N_{V} , we are not able to disprove the minimum metallic conductivity approach with the drift-mobility measurements. However, σ_{min} offers no further insight into why the band mobilities are fairly independent of the material variations summarized in figure 1.

The bandtail multiple-trapping equations can also be obtained from a ‘pure-hopping’ calculation that does not invoke mobility edges (Silver *et al* 1982, Monroe 1991, Shklovskii *et al* 1989). The calculations have an important virtue in that they account for an experimental

effect at very low temperatures ('hopping down') that does not emerge from the calculations based on mobility edges. The hopping models generally assume a constant radius a for the wavefunction of the localized states, and the value that emerges for the effective band mobility is about $\mu_0 \approx \nu a^2 / k_B T$. Given the variability in the experimental estimates for ν , this model again seems unlikely to produce a near-constant magnitude for μ_0 that is independent of the materials variations.

4.2. High-temperature estimates of μ_0

We return to the difference between the low-temperature and the high-temperature estimates of μ_0 . The high-temperature drift mobilities are not dispersive; they have a modest residual temperature dependence that is fitted adequately by the form $\mu_0(1 - T_0/T)$, and it is the values of μ_0 from this expression that were plotted to represent the high-temperature experiments in figure 1. As noted earlier, existent trapping models for the high-temperature mobility do not incorporate the temperature dependence of the bandtail width. While more intricate trapping models may be envisioned, our judgment is that these are unlikely to account satisfactorily for the near constancy of the low-temperature estimates for μ_0 , and the remarkably reproducibility of the high-temperature experiments, over a substantial range of materials and bandtail distributions.

We therefore offer an alternative speculation, which is that the temperature dependence of the drift mobility μ_D at high temperatures measures an intrinsic property of the band mobility $\mu_0(T)$ in non-crystalline materials, presumably originating with the same electron-phonon coupling mechanism that accounts for the temperature-dependent bandtail width at high temperatures. At lower temperatures the bandtail width is frozen in, which may account for the success of assuming a temperature-independent value of μ_0 around $1 \text{ cm}^2 \text{ V}^{-1} \text{ s}^{-1}$ in this regime. This picture is not an obvious prediction of the familiar analytical theories (minimum-metallic conductivity or hopping models). Recent advances in the computational modelling of electronic states near a mobility edge (see Li and Drabold 2003) do offer hope for further theoretical insight into bandedge transport in non-crystalline materials.

4.3. Emission prefactor ν

Finally, we comment on the unexpected variation in the attempt-to-escape frequency ν for holes, where a reduction in the bandtail width due to the onset of crystallinity apparently caused a large reduction in the value of ν . For deep traps, Yelon and Movaghar (2002) have noted the spectacular range of values for ν that have been inferred from experiment, and suggested that this range reflects the need to emit several phonons when a carrier is trapped. Chen *et al* (1997) have discussed how variations in the emission prefactor ν for differing states within the bandtail would affect drift-mobility measurements; the usual trapping models assume a single, constant value of this prefactor for all bandtail states.

We speculate that variations in the multiple-trapping fitting parameter ν primarily reflect changes in the density of states N_V at the transport edge. With this interpretation, the decline in ν as the crystalline volume fraction increases in $\mu\text{C-Si:H}$ would indicate a lowering of the value for N_V .

Some justification for this viewpoint emerges from the 'detailed balance' relationship $\nu = N_V b_T$, where b_T is the capture coefficient describing the rate of capture of a free hole onto a bandtail trap. Detailed balance is used in the derivation of the bandtail multiple-trapping equations (3). It is conceivable that b_T does not vary strongly between different materials, in which case the variation in ν would be mostly attributable to variation in N_V . For example,

a diffusion-limited capture expression for b_T is written $b_T = 2\pi(k_B T \mu_0)a$, where a is the capture radius of a trap; there is nothing about a that suggests a several-order-of-magnitude variation between materials.

4.4. Summary

In summary, we have presented a unified analysis of most published electron and hole drift-mobility measurements on hydrogenated amorphous silicon, amorphous silicon–germanium, amorphous silicon–carbon, and microcrystalline silicon. We analyse low-temperature, dispersive measurements using a single version of the well known exponential bandtail trapping model; we find that measurements on a very wide range of materials suggest a ‘universal’ value for the band mobility near $1 \text{ cm}^2 \text{ V}^{-1} \text{ s}^{-1}$. We discuss the hopping and minimum-metallic conductivity models, and conclude that these do not account for this value or its apparent universality. We show that high-temperature, non-dispersive drift-mobility measurements on a-Si:H are very reproducible. We discuss trapping models for these measurements, but suggest an alternative possibility that the high-temperature measurements reflect the band mobility’s dependence on the same processes as lead to temperature-dependent bandtail widths in the high-temperature regime. We note that low-temperature estimates of the attempt-to-escape frequency ν for holes trapped by the valence bandtail indicate that ν declines by about 1000 as amorphous silicon is transformed into microcrystalline silicon; we speculate that this decline is due to a comparable decline in the effective density of states N_V at the valence band mobility edge.

Acknowledgments

This research was supported by the US National Renewable Energy Laboratory (NDJ-2-30630-24). The author thanks D Drabold (Ohio University) for helpful correspondence. This work was only possible because of collaborations with the many scientists who are acknowledged in the references.

References

- Aljishi S, Cohen J D, Jin S and Ley L 1990 *Phys. Rev. Lett.* **64** 2811
 Arkhipov V I and Rudenko A I 1982 *Phil. Mag.* **B 45** 189
 Atta-Fynn R, Biswas P, Ordejon P and Drabold D A 2004 *Phys. Rev. B* **69** 085207
 Bayley P A and Marshall J M 1996 *Phil. Mag.* **B 73** 429
 Brinza M, Emelianova E V, Stesmans A and Adriaenssens G J 2004 *Amorphous and Microcrystalline Silicon Science and Technology (Materials Research Society Symp. Proc. vol 808)* ed G Ganguly, M Kondo, E A Schiff, R Carius and R Biswas (Pittsburgh, PA: Materials Research Society) p 85
 Chen W C and Hamel L-A 1996 *Amorphous Silicon Technology 1996 (Materials Research Society Symp. Proc. vol 420)* ed M Hack, E A Schiff, S Wagner, R Schropp and A Matsuda (Pittsburgh, PA: Materials Research Society) p 759
 Chen W C, Hamel L-A and Yelon A 1997 *J. Non-Cryst. Solids* **220** 254
 Cody G D, Tiedje T, Abeles B, Brooks B and Goldstein Y 1982 *Phys. Rev. Lett.* **47** 1480
 Devlen R I, Tauc J and Schiff E A 1989 *J. Non-Cryst. Solids* **114** 567
 Dinca S, Ganguly G, Lu Z, Schiff E A, Vlahos V, Wronski C R and Yuan Q 2003 *Amorphous and Nanocrystalline Silicon Based Films–2003 (Materials Research Society Symp. Proc. vol 762)* ed J R Abelson, G Ganguly, H Matsumura, J Robertson and E A Schiff (Pittsburgh, PA: Materials Research Society) p 345
 Dylla T 2004 *Doctoral Dissertation* Freie Universität Berlin, unpublished
 Dylla T, Finger F and Schiff E A 2004 *Amorphous and Microcrystalline Silicon Science and Technology (Materials Research Society Symp. Proc. vol 808)* ed G Ganguly, M Kondo, E A Schiff, R Carius and R Biswas (Pittsburgh, PA: Materials Research Society) p 109

- Ganguly G, Sakata I and Matsuda A 1995 *J. Non-Cryst. Solids* **198–200** 300
- Gu Q, Schiff E A, Chevrier J-B and Equer B 1995 *Phys. Rev. B* **52** 5695
- Gu Q, Wang Q, Schiff E A, Li Y-M and Malone C 1994 *J. Appl. Phys.* **78** 2311
- Hourd A C and Spear W E 1985 *Phil. Mag.* **B 51** L13
- Howard J and Street R A 1991 *Phys. Rev. B* **44** 7935
- Juška G, Arlauskas K, Kočka J, Hoheisel M and Chabloz P 1995 *Phys. Rev. Lett.* **75** 2984
- Juška G, Viliūnas M, Arlauskas K, Nekrašas N, Wyršch N and Feitknecht L 2001 *J. Appl. Phys.* **89** 4971
- Könenkamp R 2000 *Photoelectric Properties and Applications of Low-Mobility Semiconductors* (Berlin: Springer)
- Li J and Drabold D 2003 *Phys. Rev. B* **68** 33103
- Liu E Z, Pang D, Paul W and Chen J H 1992 *Amorphous Silicon Technology—1992 (Materials Research Society Symp. Proc. vol 258)* ed M J Thompson, Y Hamakawa, P G LeComber, A Madan and E A Schiff (Pittsburgh, PA: Materials Research Society) p 529
- Longeaud C and Vanderhagen R 1990 *Phil. Mag.* **B 61** 277
- Marshall J M 1989 *Amorphous Silicon and Related Materials* vol B, ed H Fritzsche (Singapore: World Scientific) p 799
- Marshall J M, Street R A and Thompson M J 1986 *Phil. Mag.* **B 54** 51
- Monroe D 1991 *Hopping Transport in Solids* ed M Pollak and B I Shklovskii (New York: Elsevier) p 49
- Moon J A, Tauc J, Lee J-K, Schiff E A, Wickboldt P and Paul W 1994 *Phys. Rev. B* **50** 10608
- Mott N F 1987 *Conduction in Non-Crystalline Solids* (Oxford: Oxford University Press)
- Nampoothiri A V V, Nelson B P and Dexheimer S 2003 *Amorphous and Nanocrystalline Silicon Based Films—2003 (Materials Research Society Symp. Proc. vol 762)* ed J R Abelson, G Ganguly, H Matsumura, J Robertson and E A Schiff (Pittsburgh, PA: Materials Research Society) p 333
- Nebel C E 1991 *Doctoral Dissertation* Universität Stuttgart, unpublished
- Nebel C E and Bauer G 1989 *Phil. Mag.* **B 59** 463
- Nebel C E, Weller H C and Bauer G H 1988 *Amorphous Silicon Technology (Materials Research Society Symp. Proc. vol 118)* ed A Madan, M J Thompson, P C Taylor, P G LeComber and Y Hamakawa (Pittsburgh, PA: Materials Research Society) p 507
- Orenstein J, Kastner M and Vaninov V 1982 *Phil. Mag.* **B 46** 23
- Rao P N 1999 *Doctoral Dissertation* Syracuse University, unpublished
- Rudenko A I and Arkhipov V I 1982 *Phil. Mag.* **B 45** 209
- Scher H, Schlesinger M F and Bendler J T 1991 *Phys. Today* **44** (1) 26
- Schmidt J A, Hundhausen M and Ley L 2000 *Phys. Rev. B* **62** 13010
- Shklovskii B I, Fritzsche H and Baranovskii S D 1989 *Phys. Rev. Lett.* **62** 2989
- Silver M, Schönherr G and Bäßler H 1982 *Phys. Rev. Lett.* **48** 352
- Street R A 1991 *Hydrogenated Amorphous Silicon* (Cambridge: Cambridge University Press)
- Street R A, Kakalios J and Hack M 1988 *Phys. Rev. B* **38** 5603
- Thorpe M F and Weaire D 1971 *Phys. Rev. B* **4** 3518
- Tiedje T 1984 *Hydrogenated Amorphous Silicon* vol 2, ed J D Joannopoulos and G Lucovsky (New York: Springer) pp 261–300
- Tiedje T, Cebulka J M, Morel D L and Abeles B 1981 *Phys. Rev. Lett.* **46** 1425
- Wang Q, Antoniadis H, Schiff E A and Guha S 1993 *Phys. Rev. B* **47** 9435
- Weaire D and Thorpe M F 1971 *Phys. Rev. B* **4** 2508
- Yelon A and Movaghar B 2002 *Phys. Rev. B* **65** 077202